Multi-String Capacitively Isolated Quasi- Resonant LED Driver

A. Bazarov, A. Abramovitz, D. Shmilovitz
Dept. of Physical Electronics, School of Electrical Engineering, Faculty of Engineering, Tel-Aviv University, Tel-Aviv, Israel, 69978. E-mail: shmilo@post.tau.ac.il

***Abstract*- This paper introduces a multi-string quasi-resonant driver for LED lighting applications. The proposed LED driver is operated with variable frequency, constant on-time control strategy. Key characteristics of the proposed driver under the proposed control method are reported. The theory is verified by simulation and experimental results.**

***Index Terms*—LED driver, capacitive isolation, quasi resonant conversion, PFC.**

I. Introduction

Recent years have seen major advances in LED semiconductor technology which have resulted in improved brightness and color temperature, lower energy consumption, and longer life spans in LED light sources [1] - [5]. Offline LED lighting systems will gradually replace the existing solutions. However, off-line operation of LED luminaries presents numerous challenges. First is the required ac to dc conversion with a large voltage step down while presenting a high power factor (PF) to the power system [3], [6] - [7]. Moreover, LEDs are nonlinear loads with steep current–voltage characteristics. Therefore they should be energized by a current source (whereas the input is a voltage source). This calls for driver circuits with gyrator characteristics (on average) [8], [9]. Isolation is also desired for safety reasons. Isolation transformers are difficult to manufacture automatically. Avoiding the use of an isolation transformer, potentially, can offer better compliance with machine mass production techniques.

Line isolation by means of capacitive coupling was attempted by [10], [11]. This entails using two capacitors placed on the "go" and the "return" bus lines. These series capacitors are sufficiently small to prevent shock hazard, yet, provide capacitive power transfer. Additional discussion of the safety issues of capacitive isolation can be found in [10].

Recently, a family of single stage, single switch, low-cost Quasi-Resonant offline LED Drivers (QRLEDD) with capacitive isolation barrier have been introduced [12], [13]. The previous study [14] revealed that under variable frequency constant duty cycle control, the operational characteristics of the QRLEDD were highly nonlinear and posed several design challenges. An additional limitation was the high voltage stress on the power switch. These shortcomings motivated further investigation. The present study suggests a modification of the earlier topology to a multi-string version as well as application of a different control strategy- the variable frequency constant on-time control. The undertaken control approach offers better performance in terms of reduced stress. Another prominent feature of the proposed topology is the capacitively isolated inherently balanced LED strings outputs. Analytical derivations were confirmed by simulation and experimental results.

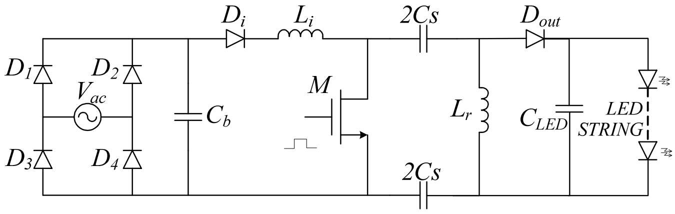

Fig. 1. Proposed capacitively isolated Quasi Resonant LED Driver.

II. Single String QRLEDD

The topology of the single string QRLEDD is shown in Fig. 1. The proposed QRLEDD is comprised of a low frequency bridge rectifier D_1-D_4, with a small high-frequency bypass capacitor, C_b, on its dc port. The input inductor, L_i, is switched by the switch, M, to shape and control the magnitude of the input current. Fast input diode D_i, in series with L_i assures unidirectional energy flow. The capacitive isolation barrier is created by a pair of small series blocking capacitors, $2C_s$. The diode D_{out} serves as output rectifier. The load is comprised of a string of LEDs connected across the filter capacitance, C_{LED}.

The QRLEDD has a merit of a single ground referenced switch and gate driver. The switch can operate at high frequency due to zero current turn-on and zero voltage switching turn-off conditions inherently created by the circuit. Blocking capacitors are also used as a part of resonant circuit. Another prominent feature of the QRLEDD is its resistive input port characteristics, which stems from discontinuous current mode operation of the input inductor.

III. Analysis

A. Basic Assumptions

To simplify the analysis the following assumptions are adopted: a) the QRLEDD operates in the quasi-steady state equilibrium in the vicinity of a certain value of the input voltage, V_i, which is considered constant; b) the operating voltage of the LED string, V_{LED}, is constant, thus, the LED string and the associated filter capacitance, C_{LED}, can be represented by an equivalent dc voltage source; c) the equivalent capacitor, C_s, represents the pair of series blocking capacitors; d) all the semiconductors operate as ideal switches. The resulting model is shown in Fig. 2 (a). The detailed steady state waveforms are presented in Fig. 2 (b). Examining the switch waveforms in Fig. 2 (b) reveals favorable zero voltage (ZV) turn off and zero current (ZC) turn on switching of the MOSFET switch, which can help to attain high efficiency at high frequency. The simulated average line current waveform, i_{ac}, shown in Fig. 2 (c) appears as a near sinusoidal signal, which manifests that the QRLEDD possesses inherently high power factor and low harmonic content.

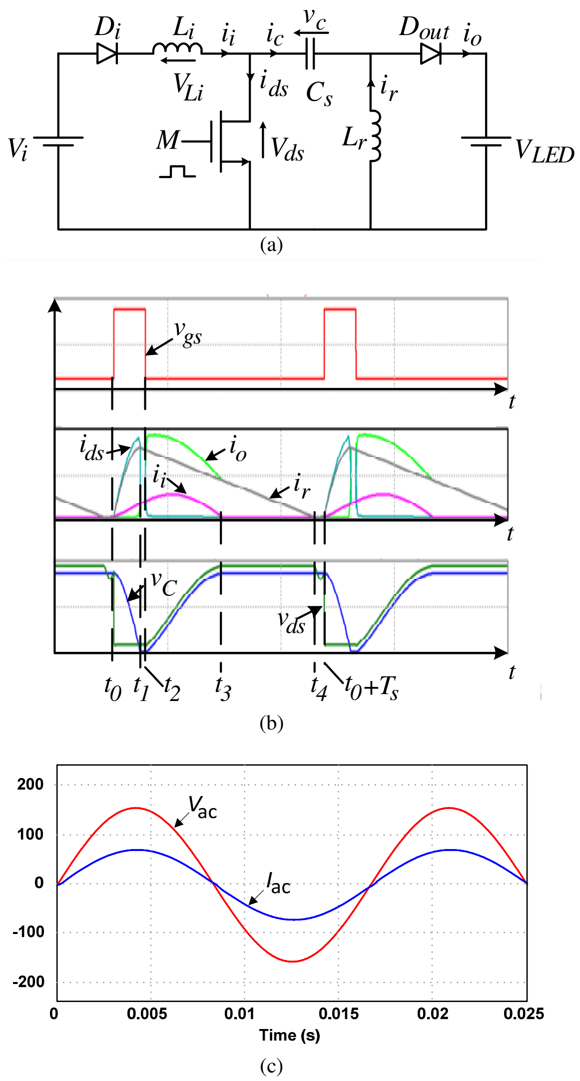

Fig. 2. The proposed QRLEDD in the steady state: (a) simplified equivalent circuit; (b) key simulated waveforms on the switching period scale; (c) on the line cycle scale: outer-the line voltage, v_{ac}, inner – the average line current, i_{ac}.

B. State Analysis

Analysis of the QRLEDD waveforms in Fig. 2 (b) revealed that the high frequency switching cycle of QRLEDD has five topological states. The state's equivalent circuits are show in Fig. 3.

State A: t_0-t_1, see Fig. 3 (a), commences when M is turned on. The switching occurs at zero current condition. Here, L_i begins charging from the input source, V_i, via D_i, while C_s and L_r resonate.

State B: t_1-t_2, see Fig. 3 (b), commences as D_{out} conducts and establishes a discharge path for L_r to the output, V_{LED}, while clamping C_s to the negative of the output voltage. Since M is still on, the inductor L_i keeps charging.

State C: t_2-t_3, see Fig. 3 (c), commences when the switch, M, is turned off, which occurs at zero voltage, v_{ds}=0, thanks to C_s snubbing. As L_i and C_s start resonating the capacitor C_s is charged to high voltage while the diode D_{out}, conducts the resonant current to the output. Here, L_r is clamped to the output and discharges. State C ends as the inductor L_i is discharged and the diode, D_i, turns off at zero current.

State D: t_3-t_4, see Fig. 3 (d), commences upon the turn off of the diode D_i. The inductor, L_r, continues to discharge its stored energy to the output. Meanwhile the capacitor, C_s, preserves its state. When the inductor, L_r, is totally discharged, the diode, D_{out}, turns off at zero current and terminates State D.

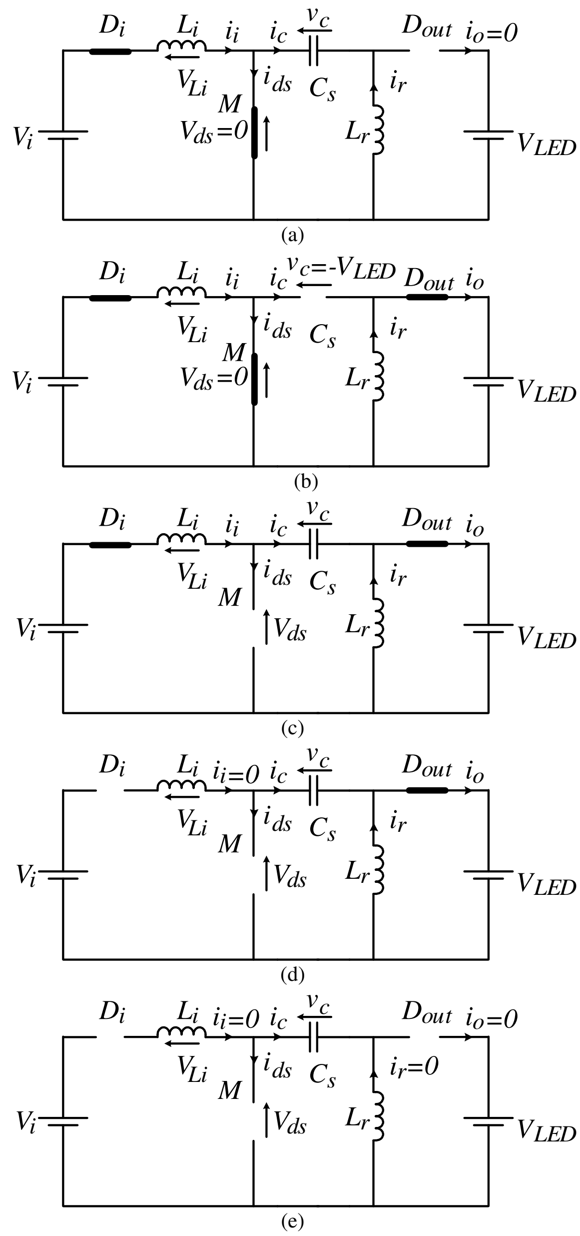

Fig. 3. Equivalent circuits of the topological states of the proposed QRLEDD. (a) State A; (b) State B; (c) State C; (d) State D; (e) State E.

State E: t_4-T_s, see Fig. 3 (e), is the idle state. Here, inductors carry no current and the capacitor, C_s, preserves its state.

C. Quantitative Analysis

1) Switch Voltage Stress

During State D the diode D_{out} conducts, see Fig. 3 (d), and imposes the sum of the peak capacitor voltage, V_m, and the output voltage, V_{LED}, to appear across the switch. The normalized peak switch voltage, V_{dsmn}, is given by

$$V_{dsmn} = \frac{V_{dsm}}{V_i} = \frac{V_m+V_{LED}}{V_i} = 1 + \sqrt{1+\left(\frac{\pi}{2r}T_{on\_n}\right)^2} \qquad (1)$$

where $r^2 = L_i/L_r$ is the inductor ratio, and the normalized on time, $T_{on\_n} = 2T_{on}/\pi\sqrt{L_rC_s}$, is defined relatively to quarter of a resonant cycle of the L_r-C_s branch.

The normalized peak switch voltage (1) is plotted on Fig. 4 as function of the normalized on time, T_{on_n}, and inductor ratio r^2. Note that the switch peak voltage is independent of the switching frequency. The output power of QRLEDD can be adjusted modulating the switching frequency. Hence, the fact that frequency variations have no effect on switch voltage stress is an operational advantage of the constant T_{on} control strategy.

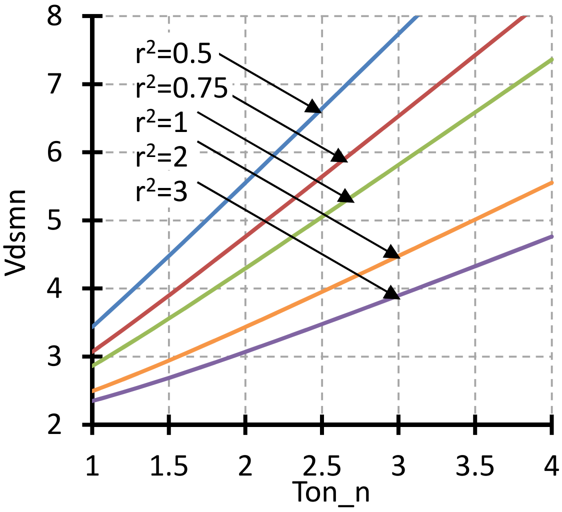

Fig. 4. Plot of the normalized peak switch voltage, V_{dsmn}, for different values of T_{on_n} and r^2.

2) Output Power

In the steady state, the average output power, P_{LED}, per switching cycle, T_s, can be found according to

$$P_{LED} = \frac{C_s}{T_s}\left[V_{LED}(V_m + V_{LED}) + \frac{(V_m^2-V_{LED}^2)}{2}\right] = f_sC_s\frac{V_{dsm}^2}{2} \qquad (2)$$

where, f_s is the switching frequency.

Combining (2) and (1) the emulated resistance, R_e, at the QRLEDD input port can be found as

$$R_e = \frac{{V_i}^2}{P_{LED}} = \frac{2}{f_s\, C_s\, V_{dsmn}^2} \qquad (3)$$

The normalized output power, P_n, can be obtained manipulating (2)

$$P_n = \frac{P_{LED}}{\left(\frac{{V_i}^2}{Z_{0i}}\right)} = \left(\frac{f_n}{4\pi}\right)V_{dsmn}^2 \qquad (4)$$

where, $f_n = \frac{f_s}{f_{0s}}$ is the normalized switching frequency, $f_{0s} = \frac{1}{2\pi\sqrt{L_iC_s}}$ is the resonant frequency and $Z_{0i} = \sqrt{\frac{L_i}{C_s}}$ is the characteristic impedance of the L_i-C_s branch .

3) Switch Current Stress

The approximated expression for the normalized switch rms current can be found as

$$I_{ds\_rms\_n} = \frac{I_{ds\_rms}}{V_i/Z_{0i}} = \left[f_n\left(\frac{r}{8}(V_{mn}^2 - V_{Ln}^2) + \frac{\pi^2}{24}\left(\frac{T_{on\_n}}{r}\right)^3\right)\right]^{1/2} \qquad (5)$$

where, $V_{Ln} = V_{LED}/V_i$ is the normalized LED string voltage, $V_{mn}=V_m/V_i$ is normalized V_m and T_{on_n}, Z_{0i} and f_n as defined above.

4) AC Operation of QRLEDD

Recall that the analysis above was performed under the assumption that the input voltage to QRLEDD, V_i, is held constant, thus (2) and (4) are valid for dc operation conditions. When QRLEDD is operated off the utility line additional considerations apply.

Assuming the QRLEDD operates in the quasi-steady state regime throughout the line period with fixed T_{on} and f_s the emulated resistance, R_e, (3) is also holds for AC input. Accordingly, the average power at QRLEDD input port is

$$P_{AC} = \frac{{V_{rms}}^2}{R_e} = \frac{1}{2}\frac{{V_i}^2}{R_e} = \frac{1}{2}P_{LED} \qquad (6)$$

here V_i stands for the ac line amplitude and the corresponding line rms voltage is $V_{rms} = \frac{1}{\sqrt{2}}V_i$.

The normalized ac power can be written as follows

$$\mathrm{P_{acn}} = \frac{\frac{1}{2}P_{LED}}{\frac{1}{2}{\mathrm{V_i}}^2/\mathrm{Z_{0i}}} = \frac{P_{AC}}{{\mathrm{V_{rms}}}^2/\mathrm{Z_{0i}}} = \left(\frac{f_n}{4\pi}\right)V_{dsmn}^2 = \mathrm{P_n} \qquad (7)$$

which is identical to (4).

Since for a constant on time, T_{on_n}, the peak switch voltage, V_{dsmn}, (1), is fixed, the output power (7) is linear with the normalized switching frequency, f_n. This is an additional advantage of the constant T_{on} control strategy.

IV. Multi-String QRLEDD

The straightforward solution for driving a number of LED strings is connecting *n* QRLEDD units in parallel. However, a more economical solution can be found. The proposed multi-string (MS) version of the QRLEDD is shown in Fig. 5.

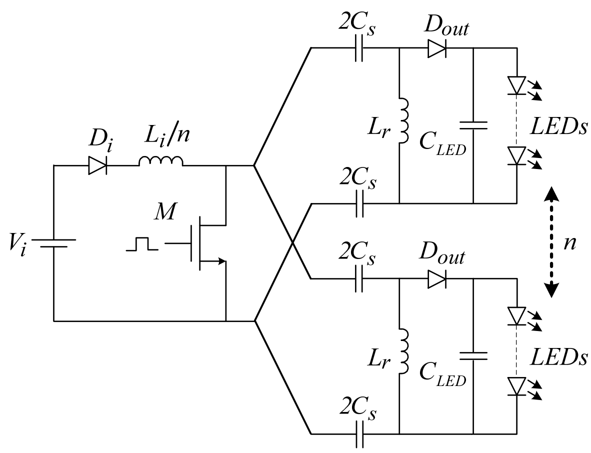

Fig. 5. The proposed multi-string QRLEDD topology.

Here a common input semi-stage is driving an appropriate number of output semi-stages. The output semi-stages are isolated from one another by capacitive isolation barrier. Since the output semi-stages are identical, same power is delivered to each LED string. A simplified model of the multi-string QRLEDD is shown in Fig. 6. The model represents n QRLEDDs connected in parallel. For this reason the input inductor value is set to L_i/n, while the equivalent output semi-stage consists of equivalent capacitor nC_s and the equivalent output inductor L_r/n. The equivalent model in Fig. 6 is identical to the single string model in Fig. 2 (a) and, therefore, same theoretical predictions, albeit with the aforementioned equivalent values, can be used for analysis and design of the circuit.

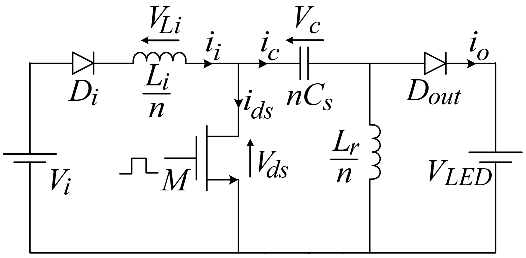

Fig. 6. Simplified model of the multi-string QRLEDD.

V. Simulation and Experimental Verification

To further verify the theoretical predictions, a 3x20W, 110Vac-input experimental multi-string QRLEDD prototype in Fig. 6 was built and tested. The circuit parameters were: maximum switching frequency f_s=130 kHz; input inductance $L_i/3$=79 µH; the resonant inductors: $L_{r1}=L_{r2}=L_{r3}$=79 µH; capacitors: $2C_S$=8 nF; C_b=540 nF; C_{LED}=220 µF, V_{LED}=29 V @0.7 A (20.3 W).

Key waveforms of the experimental prototype are shown in Fig. 7 (a) and (b). Experimental waveforms in Fig. 7 (a) confirm that zero current switching at turn on of the switch and zero voltage switching at turn off of the switch were achieved. Moderate ringing can be noticed in the v_{ds} waveform. Stray inductances of the current probe loop result in current ringing that can be observed in i_{ds} waveform.

The measured average ac line current of QRLEDD, is shown in Fig. 8 and is of an excellent quality in the power range of interest somewhat deteriorating at low power level.

The input and output power of the multi-string QRLEDD operated from a dc source is shown in Fig. 9 (a) and stanfs in good agreement with the theoretical prediction. The efficiency plot is given in Fig. 9 (b).

As can be seen in Fig. 10, the experimental multi-string QRLEDD inherently attained excellent power balance in between the all three LED strings without implementing active control of the LED current.

Measured power of the experimental multi-string QRLEDD at different switching frequencies, f_s, (and power level) operated from ac line is shown in Fig. 11 (a) in comparison with the theoretical prediction. The efficiency plot is given in Fig. 11 (b) and is somewhat lower than one measured in dc conditions.

Comparison of calculated and measured emulated resistance, R_e, for ac and dc inputs is shown in Fig. 12. Excellent agreement is found.

The multi-string QRLEDD excels in its power factor and the total harmonic distortion performance. The experimental results are illustrated in Fig. 13.

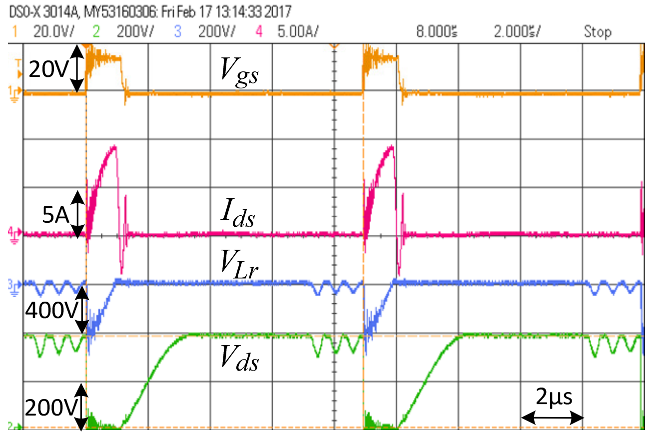

(a)

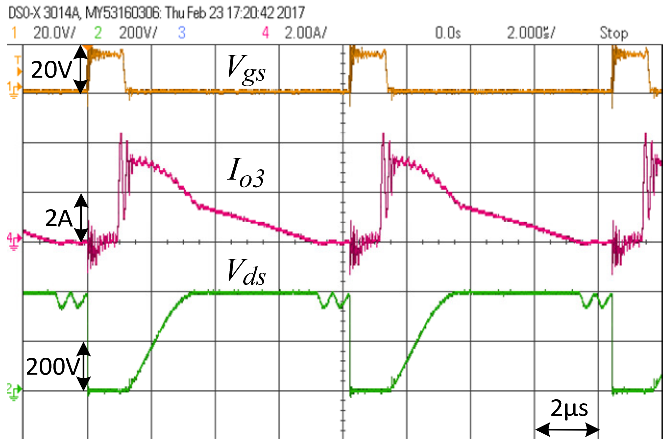

(b)

Fig. 7. Experimental results of the MS QRLEDD: typical view of the key waveforms at the switching frequency scale @ Vi=155Vdc: (a) v_{gs}, i_{ds}, v_{Lr}, v_{ds}; (b) v_{gs}, i_o, v_{ds}.

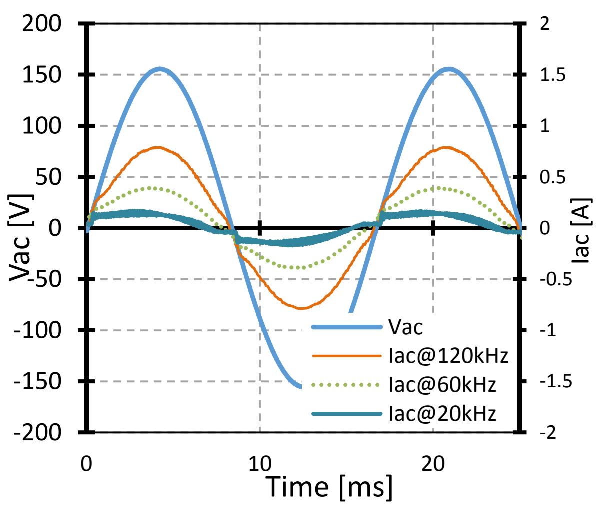

Fig. 8. Measured the ac line voltage v_{ac} and the average ac line current, i_{ac}, at different power levels (switching frequencies).

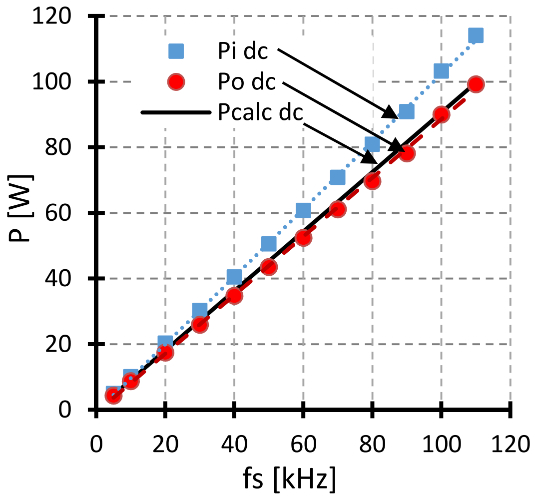

(a)

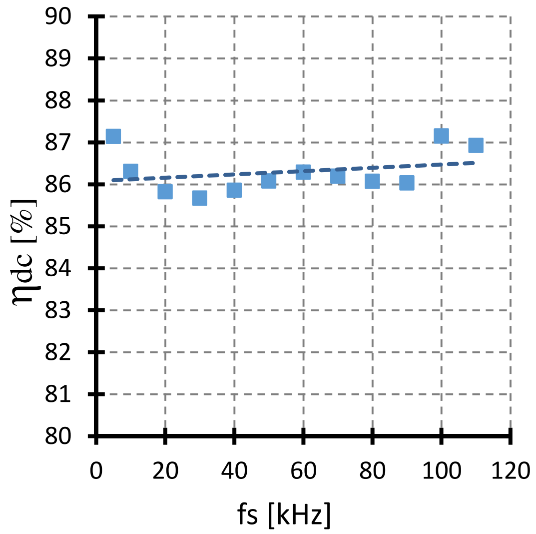

(b)

Fig. 9. Experimental results of the MS QRLEDD operated from a dc source: (a) comparison of the measured input and output powers vs. the theoretically predicted power; (b) measured efficiency.

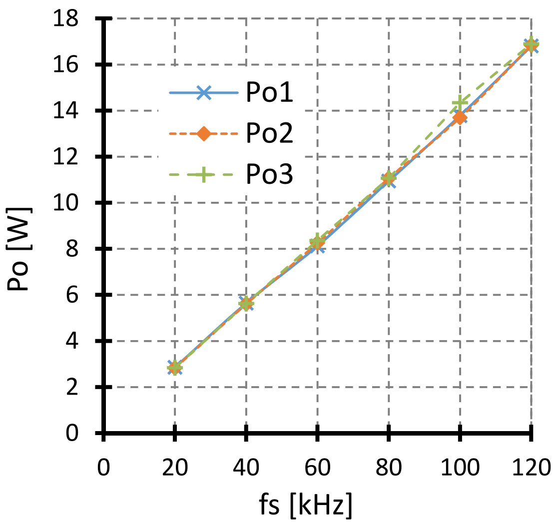

Fig. 10. Experimental results of the MS QRLEDD: power balance in between the LED strings.

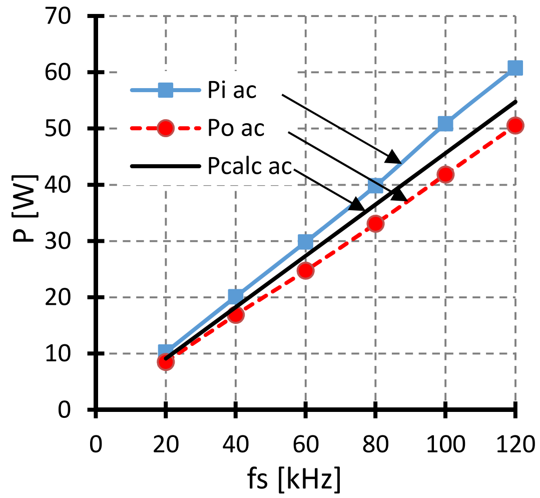

(a)

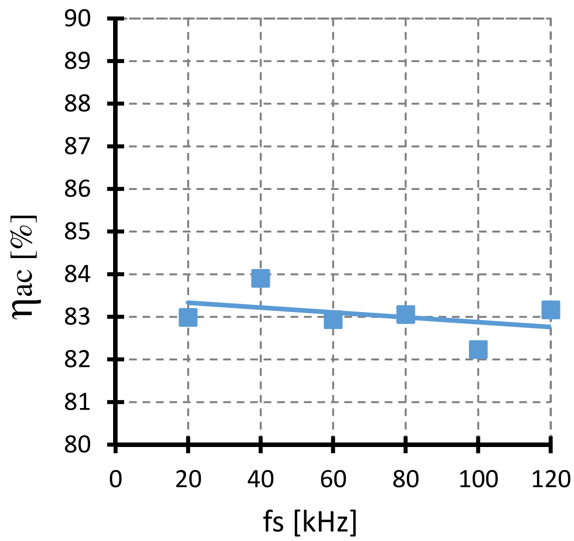

(b)

Fig. 11. Experimental results of the MS QRLEDD operated from ac line: (a) comparison of the measured input and output powers vs. the theoretically predicted power; (b) measured efficiency.

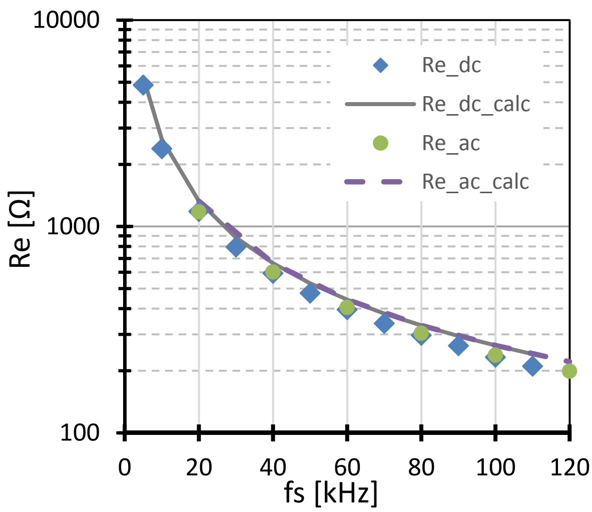

.

Fig. 12. Comparison of the measured vs. calculated equivalent input resistance, R_e, for ac and dc inputs.

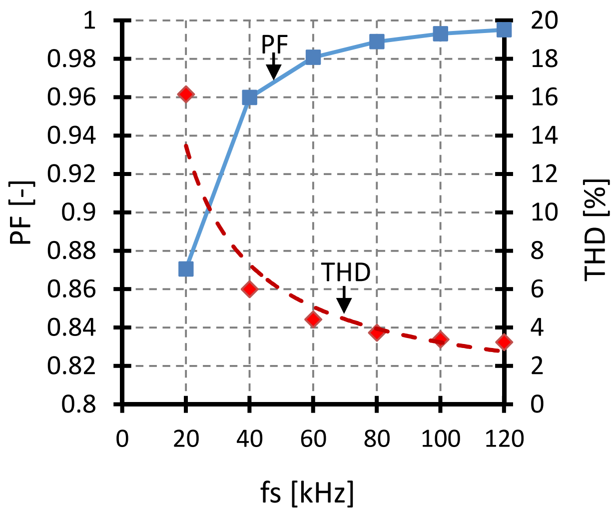

Fig. 13. Experimental results of the MS QRLEDD: (a) the power factor (PF) and the total harmonic distortion (THD) performance indices at different power levels.

VI. Conclusion

This paper introduces the variable frequency constant on time controlled quasi-resonant multi-string driver for high brightness LED lighting applications. The important merits of the proposed topology are capacitive isolation, soft switching features, high frequency operation, low line current distortion, and inherent self balancing of the LED string loads. The brightness of a LED lamp can be controlled by modulating either the switch on time, the switching frequency or applying burst strategy. Major performance indexes were derived theoretically and verified by both simulation and experiment. Good agreement was found.

References

[1] Tsao, J. Y., "Solid-state lighting: lamps, chips, and materials for tomorrow," *Circuits and Devices Magazine, IEEE*, vol.20, no.3, pp.28,37, May-June 2004.

[2] Craford, M. G., "LEDs challenge the incandescents," *Circuits and Devices Magazine, IEEE*, vol.8, no.5, pp.24,29, Sept. 1992.

[3] A. Ayachit, V. P. Galigekere, M. K. Kazimierczuk "Power Electronic Circuitry In LED Modules: An Overview," December 2011, pp. 1-11. http://www.how2power.com/newsletters/1112/index.html

[4] Yang Lu; Czarkowski, D.; Bury, W.E., "High efficiency adaptive boost converter for LED drivers," *Compatibility and Power Electronics (CPE), 2011 7th International Conference-Workshop*, pp.315-318, 1-3 June 2011

[5] Leon-Masich, A.; Valderrama-Blavi, H.; Bosque, J.M.; Cid-Pastor, A.; Martinez-Salamero, L., "High-voltage LED-based efficient lighting using a hysteretic controlled boost converter," *Compatibility and Power Electronics (CPE), 2011 7th International Conference-Workshop*, pp.439,444, 1-3 June 2011.

[6] Gacio, D., Alonso, J.M., Calleja, A.J., Garcia, J., Rico-Secades, M., "A Universal-Input Single-Stage High-Power-Factor Power Supply for HB-LEDs Based on Integrated Buck–Flyback Converter," *Industrial Electronics, IEEE Transactions on*, vol.58, no.2, pp.589,599, Feb. 2011.

[7] Jovanovic, M.M.; Hopkins, Douglas C.; Lee, F.C.Y., "Evaluation and design of megahertz-frequency off-line zero-current-switched quasi-resonant converters," Power Electronics, IEEE Transactions on , vol.4, no.1, pp.136,146, Jan 1989.

[8] S. Singer, “Gyrators application in power processing circuits,” *IEEE Trans. Ind. Electron.*, vol. IE-34, no. 3, pp. 313–318, Aug. 1987.

[9] D. Shmilovitz, I. Yaron, and S. Singer, “Transmission-line-based gyrator,” *IEEE Trans. Circuits Syst. I, Fundam. Theory Appl.*, vol. 45, no. 4, pp. 428–433, Apr. 1998.

[10] Jingpeng Zhu, Ming Xu, Julu Sun, Chuanyun Wang, "Novel capacitor-isolated power converter," in *Energy Conversion Congress and Exposition (ECCE), 2010 IEEE* , vol., no., pp.1824-1829, 12-16 Sept. 2010

[11] Huang, L., Hu, A. P., Swain, A.”A resonant compensation method for improving the performance of capacitively coupled power transfer system.” In *Energy Conversion Congress and Exposition (ECCE), 2014 IEEE* (pp. 870-875), Aug. 2014.

[12] Shmilovitz, D.; Ozeri, S.; Ehsani, M.M., "A resonant LED driver with capacitive power transfer," *Applied Power Electronics Conference and Exposition (APEC), 2014 Twenty-Ninth Annual IEEE*, pp.1384-1387, 16-20 March 2014.

[13] Richman I., Abramovitz A., Shmilovits D., "A Quasi-Resonant LED Driver with Capacitive Isolation," *Electronics Letters,* vol.51, pp.274-276, 25 2015.

[14] Shmilovitz D., Abramovitz A., Reichman I., "Quasi-Resonant LED Driver With Capacitive Isolation and High PF," *Emerging and Selected Topics in Power Electronics, IEEE Journal of* , vol.3, no.3, pp.633,641, Sept. 2015.